Research Article | Vol. 25, No. 1 | 9 Jan 2017 | OPTICS EXPRESS 271
Optics EXPRESS

# Room-temperature Fabry-Perot resonances in suspended InGaAs/InP quantum-well nanopillars on a silicon substrate

GILLIARD N. MALHEIROS-SILVEIRA, INDRASEN BHATTACHARYA, SANIYA V. DESHPANDE, DARIA SKURIDINA, FANGLU LU, AND CONNIE J. CHANG-HASNAIN*

*Department of Electrical Engineering and Computer Sciences, University of California, Berkeley, California 94720, USA.*
*cch@eecs.berkeley.edu

**Abstract:** We present a new platform based on suspended III-V semiconductor nanopillars for direct integration of optoelectronic devices on a silicon substrate. Nanopillars grown in core-shell mode with InGaAs/InP quantum wells can support long-wavelength Fabry-Pérot resonances at room temperature with this novel configuration. Experimental results are demonstrated at a silicon-transparent wavelength of 1460 nm, facilitating integration with silicon platform.



**OCIS codes:** (230.5590) Quantum-well, -wire and -dot devices; (140.4780) Optical resonators; (230.5750) Resonators; (050.2230) Fabry-Perot; (250.5230) Photoluminescence; (230.3120) Integrated optics devices.

## References and links

1. R. Chen, K. W. Ng, W. S. Ko, D. Parekh, F. Lu, T.-T. D. Tran, K. Li, and C. Chang-Hasnain, "Nanophotonic integrated circuits from nanoresonators grown on silicon," Nat. Commun. **5**, 4325 (2014).
2. G. N. Malheiros-Silveira, F. Lu, I. Bhattacharya, T.-T. D. Tran, H. Sun, and C. J. Chang-Hasnain, "Integration of III-V Nanopillar Resonator to In-Plane Silicon Waveguides," in *Conference on Lasers and Electro-Optics*, OSA Technical Digest (2016) (Optical Society of America, 2016), paper STh1L.5.
3. H. Kim, A. C. Farrell, P. Senanayake, W.-J. Lee, and D. L. Huffaker, "Monolithically Integrated InGaAs Nanowires on 3D Structured Silicon-on-Insulator as a New Platform for Full Optical Links," Nano Lett. **16**(3), 1833–1839 (2016).
4. K. Tomioka, M. Yoshimura, and T. Fukui, "A III-V nanowire channel on silicon for high-performance vertical transistors," Nature **488**(7410), 189–192 (2012).
5. M. Borg, H. Schmid, K. E. Moselund, G. Signorello, L. Gignac, J. Bruley, C. Breslin, P. Das Kanungo, P. Werner, and H. Riel, "Vertical III-V nanowire device integration on Si(100)," Nano Lett. **14**(4), 1914–1920 (2014).
6. J. Svensson, A. W. Dey, D. Jacobsson, and L.-E. Wernersson, "III-V Nanowire Complementary Metal-Oxide Semiconductor Transistors Monolithically Integrated on Si," Nano Lett. **15**(12), 7898–7904 (2015).
7. A. Brenneis, J. Overbeck, J. Treu, S. Hertenberger, S. Morkötter, M. Döblinger, J. J. Finley, G. Abstreiter, G. Koblmüller, and A. W. Holleitner, "Photocurrents in a Single InAs Nanowire/Silicon Heterojunction," ACS Nano **9**(10), 9849–9858 (2015).
8. C. P. T. Svensson, T. Mårtensson, J. Trägårdh, C. Larsson, M. Rask, D. Hessman, L. Samuelson, and J. Ohlsson, "Monolithic GaAs/InGaP nanowire light emitting diodes on silicon," Nanotechnology **19**(30), 305201 (2008).
9. I. Bhattacharya, S. Deshpande, G. N. Malheiros-Silveira, and C. J. Chang-Hasnain, "Efficient Electroluminescence from III/V Quantum-Well-in-Nanopillar Light Emitting Diodes Directly Grown on Silicon," in *Conference on Lasers and Electro-Optics*, OSA Technical Digest (2016) (Optical Society of America, 2016), paper SM4R.6.
10. W. S. Ko, I. Bhattacharya, T. D. Tran, K. W. Ng, S. Adair Gerke, and C. Chang-Hasnain, "Ultrahigh Responsivity-Bandwidth Product in a Compact InP Nanopillar Phototransistor Directly Grown on Silicon," Sci. Rep. **6**, 33368 (2016).
11. R. K. Lee, O. J. Painter, B. D'Urso, A. Scherer, and A. Yariv, "Measurement of spontaneous emission from a two-dimensional photonic band gap defined microcavity at near-infrared wavelengths," Appl. Phys. Lett. **74**(11), 1522 (1999).
12. Y. Zhang, M. Khan, Y. Huang, J. Ryou, P. Deotare, R. Dupuis, and M. Lončar, "Photonic crystal nanobeam lasers," Appl. Phys. Lett. **97**(5), 051104 (2010).

#279821 http://dx.doi.org/10.1364/OE.25.000271
Journal © 2017 Received 31 Oct 2016; revised 8 Dec 2016; accepted 12 Dec 2016; published 4 Jan 2017

13. Z. Wang, B. Tian, M. Pantouvaki, W. Guo, P. Absil, J. Van Campenhout, C. Merckling, and D. Van Thourhout, "Room-temperature InP distributed feedback laser array directly grown on silicon," Nat. Photonics **9**(12), 837–842 (2015).
14. Y. Ding, J. Motohisa, B. Hua, S. Hara, and T. Fukui, "Observation of Microcavity Modes and Waveguides in InP Nanowires Fabricated by Selective-Area Metalorganic Vapor-Phase Epitaxy," Nano Lett. **7**(12), 3598–3602 (2007).
15. S. Arab, P. D. Anderson, M. Yao, C. Zhou, P. D. Dapkus, M. L. Povinelli, and S. B. Cronin, "Enhanced Fabry-Perot resonance in GaAs nanowires through local field enhancement and surface passivation," Nano Res. **7**(8), 1146–1153 (2014).
16. F. Lu, T.-T. D. Tran, K. W. Ng, Z. Gong, and C. J. Chang-Hasnain, "Long-wavelength InGaAs/InP quantum-well-on-nanopillar laser grown on silicon," in *Compound Semiconductor Week* (2016), paper Tu4O5.3.
17. R. Chen, T.-T. D. Tran, K. W. Ng, W. S. Ko, L. C. Chuang, F. G. Sedgwick, and C. Chang-Hasnain, "Nanolasers grown on silicon," Nat. Photonics **5**(3), 170–175 (2011).
18. X. Duan, Y. Huang, R. Agarwal, and C. M. Lieber, "Single-nanowire electrically driven lasers," Nature **421**(6920), 241–245 (2003).
19. B. E. A. Saleh and M. C. Teich, *Fundamentals of Photonics*, Wiley Series in Pure and Applied Optics (John Wiley & Sons, Inc., 1991).
20. H. Ma, A. K.-Y. Jen, and L. R. Dalton, "Polymer-Based Optical Waveguides: Materials, Processing, and Devices," Adv. Mater. **14**(19), 1339–1365 (2002).
21. D. Ramos, E. Gil-Santos, V. Pini, J. M. Llorens, M. Fernández-Regúlez, Á. San Paulo, M. Calleja, and J. Tamayo, "Optomechanics with silicon nanowires by harnessing confined electromagnetic modes," Nano Lett. **12**(2), 932–937 (2012).
22. D. Ramos, E. Gil-Santos, O. Malvar, J. M. Llorens, V. Pini, A. San Paulo, M. Calleja, and J. Tamayo, "Silicon nanowires: where mechanics and optics meet at the nanoscale," Sci. Rep. **3**, 3445 (2013).

## 1. Introduction

Silicon platform has been the dominant backbone for integrated microelectronic circuits and complementary metal-oxide-semiconductor (CMOS) technology is the engine responsible for its adoption by the microelectronics industry. However, having an indirect bandgap, silicon suffers from a grave disadvantage for implementing efficient optoelectronic devices. Direct bandgap III-V compound materials are well known for the superior performance in optical processes. The monolithic integration of both platforms, such as III-V compound semiconductors onto silicon, not only allows ultra-compact optoelectronic devices, but also combines the advantages of both materials in just one platform. Mismatches of lattice constants and thermal expansion coefficients of materials are main obstacles that limit heteroepitaxial growth of thin films. The approach of growing heterostructures in nanopillars and nanowires can substantially alleviate the effects of these mismatches. Recently, semiconductor nanopillars and nanowires have been shown as ultra-compact building blocks for photonic, electronic, and optoelectronic integration to the silicon platform [1–10]. This monolithic approach has also the potential to decrease the cost of manufacturing.

In this manuscript, we start from the aforementioned monolithic integration approach when a non-native substrate is used, and we explore a new platform, inspired by suspended devices [11–13], applied to nanophotonics. As an example, we demonstrate a novel way of obtaining Fabry-Pérot (FP) modes and potentially lasing in nanopillars in long wavelength operating at room temperature, and without mechanically transferring them onto another substrate [14,15].

## 2. Materials and methods

A perspective view of the proposed platform is shown in a schematic in Fig. 1. Such a platform can be obtained by performing selective etching to remove the substrate underneath the nanopillar in order to increase the index contrast for the resonant modes from the nanopillar; increasing by consequence its quality factor, *Q*, as well as, reducing the losses down through the substrate. A structure composed by oxide is used to hold the nanopillar above the etched region of the Si substrate.

Optics EXPRESS

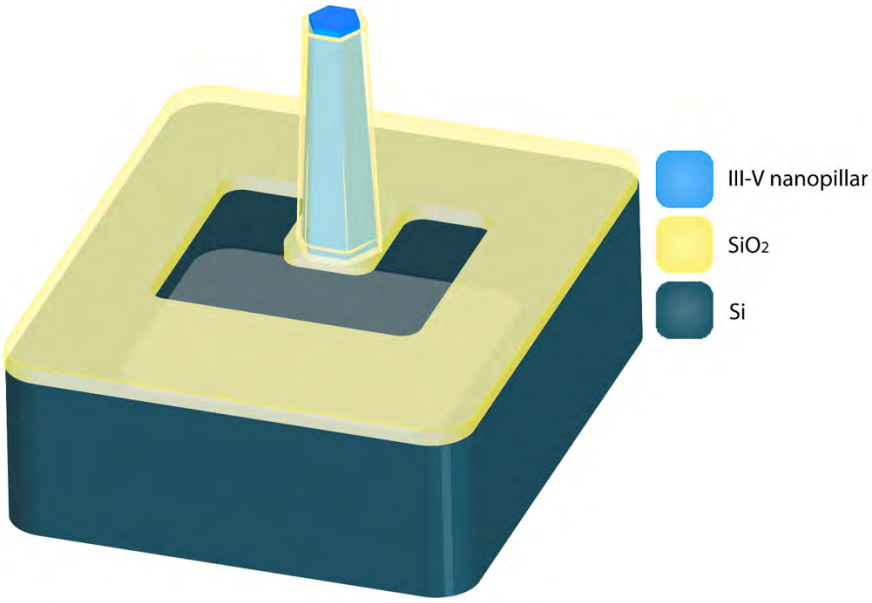


Fig. 1. Generic scheme of the proposed platform.

A core-shell configuration of InP with 3 InGaAs quantum wells (QWs) was used to evaluate this new approach of active suspended structures. InP nanopillars are grown on <111> silicon wafer by an Emcore D75; a metal-organic chemical vapor deposition (MOCVD) reactor. The growth was catalyst free and started with an InP core, followed by InGaAs QWs layers [16] spaced by InP spacer and covered by an InP layer at 455 °C. This approach was used because InP nanopillar monolithically grown on silicon can act as a template for long wavelength emission. More details of the growth process can be found in [17]. In this growth, nanopillars have a core-shell configuration, and the thickness of each layer is nearly linearly scalable with the growth time. For the actual sample, InP core and cladding were designed to assume 400 nm and 75 nm of radii, respectively. The InGaAs QWs were designed to have 5 nm of thickness, spaced by 5 nm of InP layers.

Figure 2(a) shows a scanning electron microscopy (SEM) image from as-grown InP nanopillar sample with multiple InGaAs QWs onto Si. Top inset depicts a cross-section from the III-V compound semiconductors arranged in core-shell configuration grown on top of the silicon substrate. Figure 2(b) shows the micro-photoluminescence (μ-PL) spectra, at 5 K, when the power from the laser pump operating at $\lambda_p$ = 660 nm ranges from 100 to 1000 μW. Spontaneous emission has a central wavelenth at $\lambda_0$ = 1460 nm. Because the low index contrast between the III-V nanopillar and the silicon substrate the reflection at that interface was not enough to support FP modes, specially at room temperature. That effect is even more pronounced in nanopillars or nanowires grown on native substrates. Therefore a common way of exciting FP modes in nanopillars/nanowires is by removing them from the growth substrate and transfering them to another one in order to obtain high index contrast at two very ending faces of the nanopillar/nanowire [14,15].

Optics EXPRESS

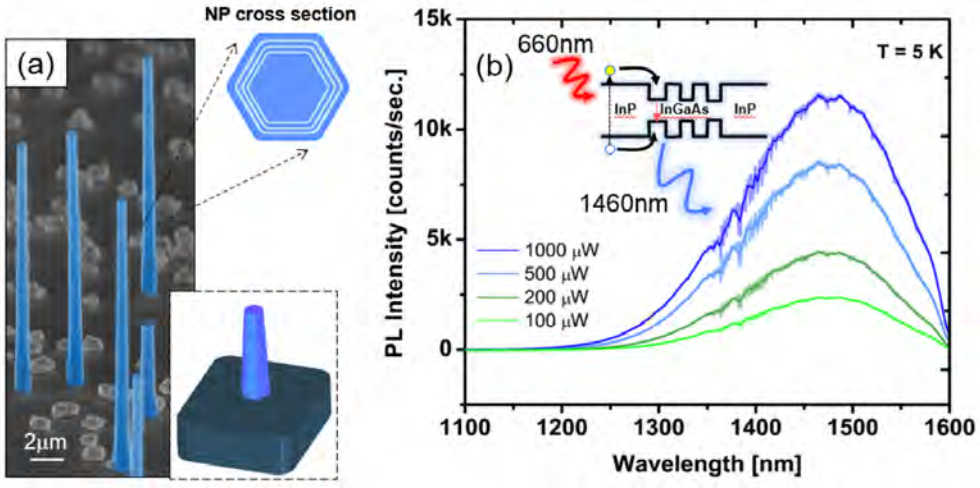


Fig. 2. (a) SEM image from nanopillars grown on top of <111> Si substrate. Inset at top-right depicts the core-shell configuration. (b) PL dependence from input power at 5 K.

Since a non-native substrate was used to grow such nanopillars we can take advantage of it by using a selective etching in order to obtain structures similar to that on depicted in Fig. 1. The layout mask of those geometries to be etched on Si, were transferred to the sample by using e-beam lithography. After developing the e-beam resist (PMMA), the exposed $SiO_2$ geometries were wet-etched by using buffered oxide etch (BOE) to expose the Si surface. Finally, a gas mixture of $SF_6$ and $O_2$ was applied in a reactive ion etching (RIE) plasma in order to etch portion of silicon underneath and nearby the nanopillar positions.

## 3. Results and discussion

Figure 3(a) shows a sketch of a structure where the nanopillar is suspended by oxide with a geometry similar to a trampoline. Figure 3(b) shows a 60° angle tilted SEM image from one of those fabricated structures. It can be seen that the nanopillar is partially covered by $SiO_2$ (only the top facet is open), and suspended by a trampoline made of $SiO_2$. Figure 3(c) highlights that silicon was completely removed underneath the nanopillar. Those geometries were obtained by over-etching silicon along the geometry defined by the $SiO_2$ mask. The final $SiO_2$ membrane had about 100 nm of thickness (estimated from the etching time), and the depth of the Si etched is about 3.8 μm (measured by 3-D laser confocal microscope) after processing the sample.

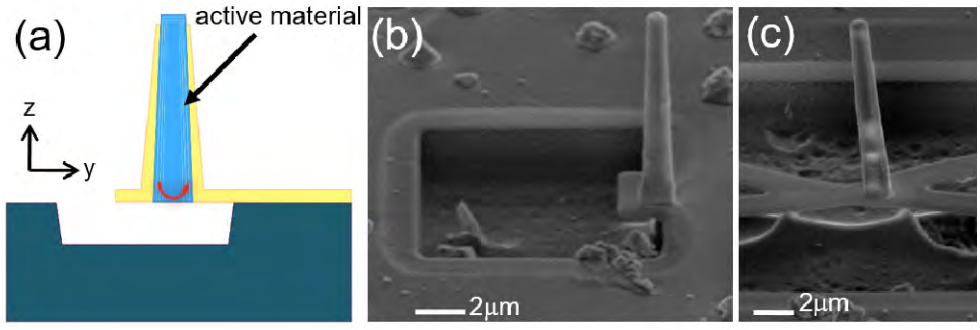


Fig. 3. (a) Sketch from a nanopillar suspended by a $SiO_2$ membrane, and isolated from the Si substrate. SEM image of 60° of tilted view from suspended structures assuming geometries of trampoline (b) and bridge (c).

Optics EXPRESS

Optical characterization of those structures was peformed by μ-PL and using CW 980 nm pump laser at room temperature (295 K). Power sweep of the spontaneous emissions from the structure shown in Fig. 3(b) is shown in Fig. 4(a). The reflection coefficient of the nanopillar is expected to increase after having a silicon portion etched underneath its bottom since the index contrast between nanopillar and air is higher than nanopillar and silicon. In fact, periodic variations in the intensity can be noticed in the spectrum which indicate longitudinal FP modes are oscilating in the cavity. FP modes excited in the nanopillar can be enhanced because of the high index contrast in its very bottom. The mode spacing, Δλ, of FP cavities is given by [18]:

$$\Delta\lambda = \frac{\lambda^2}{2L\left[n - \lambda\left(\frac{dn}{d\lambda}\right)\right]} \quad (1)$$

where $L$ is the cavity length, $n$ is the refractive index, $dn/d\lambda$ is the first-order dispersion of the refractive index, and $n_g = n - \lambda dn/d\lambda$ is the group refractive index. This equation provides a good description from the cavity once the mode spacing observed from the spontaneous emission [shown in Fig. 4(a)] can be related to the cavity length (measured from SEM) in order to unplug the group refractive index. In Fig. 4(a) the FP modes present an average of Δλ = 24 nm and full-width half maximum (FWHM) of λ = 24 nm. Figure 4(b) shows the espontaneous emission measured at 5 K, when the FP modes are even more evident.

The $Q$ of the cavity can be defined as a ratio between the mode wavelength and mode width (λ/Δλ) [19]. From our measurements the FP modes were estimated to have low $Q$s in the range of 60-80. Once it is known that $Q$ is related to cavity loss, the $Q$ can be further optimized by growing longer cavities [14]; which can be obtained by increasing the nanopillar growth time [17]. Also by reducing mirror losses; which were reduced in the very bottom of the nanopillar after applying the process proposed here. Although a larger $Q$ is required to achieve laser, the results clearly show the improvements in the reflections in the very bottom of the cavity which enhanced the FP modes at room temperature without damaging the active material. Another approach would be add more QWs in order to increase the material gain. The proposed process can benefit nanopillar lasers, as laser threshold can be decreased when the cavity $Q$ will be increased.

Optics EXPRESS

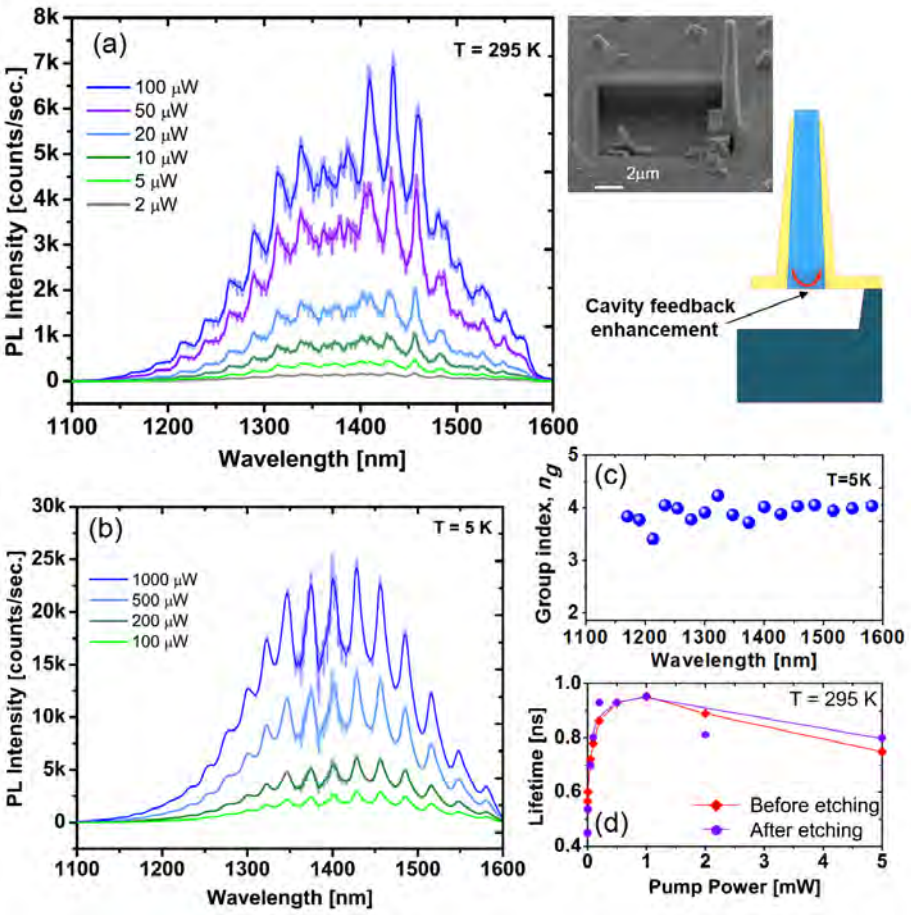


Fig. 4. Optical characterization of the proposed suspended structures. (a) Power sweeping during PL measurements at room temperature (295 K) and under CW 980 nm of laser pump. (b) PL measurements at 5 K under CW 660nm of laser pump. (c) Calculated group refractive index. (d). TRPL from a InP nanopillar before and after etching Si by using $SF_6$ plus $O_2$ RIE plasma.

Figure 4(c) shows the group refractive index calculated from Eq. (1), which assumes an average value of about 3.9 along the amplified spontaneous emission spectra. This high group index indicates that the FP modes are very well confined. A pulsed optical pumping (120 fs Ti:sapphire) operating at $\lambda_p$ = 750 nm was used to perform time- resolved photoluminescence (TRPL) measurements before and after the etching process in InP nanopillars in order to evaluate its robustness against etching. According to the results showing in Fig. 4(d) the plasma composed by $SF_6$ plus $O_2$ did not affect the optical quality from intrinsic InP nanopillars. It is also important to mention that, once InP is resistant to that plasma mixture, when eventually the $SiO_2$ covering the top region of the nanopillar gets etched, its exposure would not affect the crystal quality of the nanopillar.

Figure 5(a) shows the PL spectra for the proposed structures. The central wavelength of emission is the same even for nanopillars assuming different lengths; that fact demonstrates the uniformity of the core-shell mode growth. Also, the mode space experiences some variations as outlined in Fig. 5(b). A linear behavior relating the mode space and the inverse of the pillar lengths could be noticed from those measurements which is in strong accordance to the Eq. (1).

Optics EXPRESS

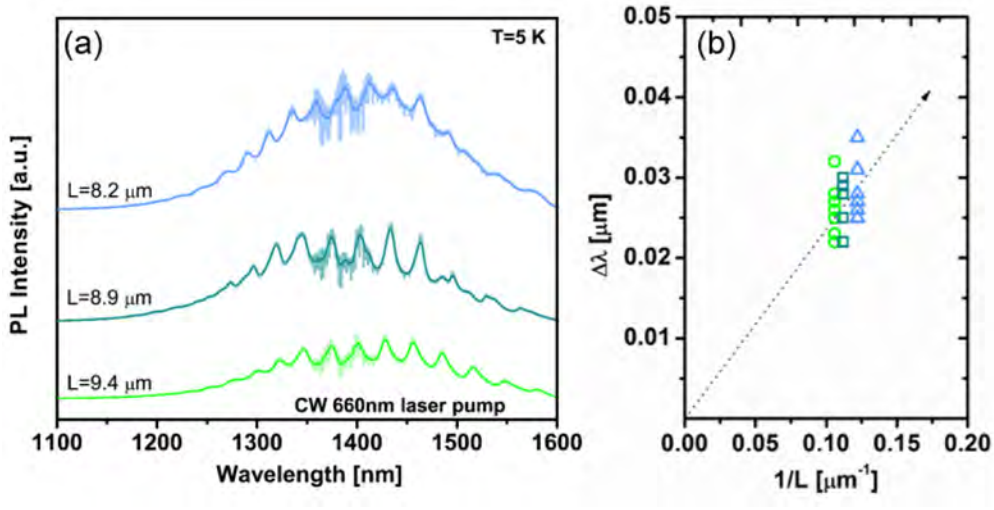


Fig. 5. (a) μ-PL spectra measured at 5 K from the three single nanopillars with different lengths at pump power of 500 μW. (b). Inverse length of the nanopillars versus mode spacing variation shows a linear dependence.

## 4. Conclusion

In conclusion, we demonstrate a feasible way of creating long-wavelength FP cavity in nanopillars at room and low temperatures. The fabrication process takes advantage of growth of nanopillars on non-native substrate, and applies selective etching in order to remove a specific region from the substrate without compromising the material quality of the nanopillar. This leads to an increasing of the reflectivity of the very bottom mirror; which by consequence allows the structure to enhance FP modes. Those FP modes can be obtained at not only low temperature, but also room temperature without using any mechanical process, and without damaging the nanopillars. This new platform can be used, for example, for sensor applications, as a source of light or an optical coupler for polymer-based optical waveguides [20], as well as, a novel platform for optomechanics based on nanopillars/nanowires [21,22]. Finally, although nanopillars were used like an example, the proposal can also be extended to nanowires.

## Funding

We acknowledge the support of grants under National Science Foundation (NSF) (0939514, 1335609).